

Advanced Topics on Erbium Doped Fibers for High Performance Amplifiers

(Invited Paper)

B. S. Wang, M. J. Andrejco*

OFS, Specialty Photonics Division, 25 Schoolhouse Road, Somerset, NJ 08873, USA,
bswang@ofsoptics.com; *OFS Laboratory, 25 Schoolhouse Road, Somerset, NJ 08873

ABSTRACT

Erbium doped fiber amplifiers have been widely deployed for signal amplification in optical transmission systems. High performance amplifiers require erbium doped fiber with high power conversion efficiency and consistent flat gain spectrum. In addition, all impairments associated with EDF must be under good control. This paper reviews the current status and recent progress on erbium doped fibers, illustrates C and L-band spectral characteristics resulting from different doping compositions, presents some approaches for efficient high power amplifiers, and discusses some EDF nonlinear effects with examples.

Keywords: erbium-doped fiber, amplifier, high power, efficiency, gain flatness, aluminum, phosphorus, temperature, pump induced inhomogeneity, impairment, splice loss

1. INTRODUCTION

Erbium-doped fiber amplifiers (EDFA) continue to be widely used in long-haul/metro transport systems and CATV applications because they offer cost effective solutions for optical amplification⁽¹⁾. High performance EDFAs require precise control of doping composition of EDFs to maintain consistent and flat EDFA spectral gain shape. This requires a thorough understanding of EDF's spectral characteristics as a function of dopant type, concentration, and waveguide design⁽²⁾. Requirements for higher power amplifiers for longer reach and wider gain dynamics pose new challenges to EDF design. In addition, EDF's non-linear effects, such as temperature dependency, pump induced inhomogeneity⁽³⁾,⁽⁴⁾, which impairs system performance, need to be well understood and under proper control.

We review the current status and recent progress of erbium doped fibers. The main focus of the paper is on the following topics.

1. Spectral characteristics of erbium doped fibers: The effect of doping composition on the spectral gain shape of the fiber is discussed. Quantitative EDF spectral data in both C-band and L-band wavelength region is provided for fibers with different aluminum concentrations and phosphorus doping.
2. High power applications: Approaches for improving amplifier performance for high power application are presented. EDF design optimization with different numerical apertures (NA) is described. An EDF design example with low NA and high aluminum concentration is shown. Results of the efficiency, spectral characteristics, and typical splice performance of this fiber with comparison with another typical C-band fiber are provided. An approach for even higher power application (>27dBm) using hybrid fibers with Er/Yb double cladding fiber is also discussed.
3. Other advanced EDF topics: For high performance amplifier design, temperature characteristics and pump induced inhomogeneity need to be understood thoroughly and controlled. These effects are reviewed with some experimental and modeling examples.

2. EDF SPECTRAL CHARACTERISTICS

It is known that doping composition plays a critical role in determining the spectral characteristics and performance of erbium doped fibers ^{(3), (4), (5), (6)}. EDFs are typically co-doped with germanium, lanthanum, aluminum, and phosphorus. Both aluminum and phosphorus dramatically affect EDF's spectral characteristics. High aluminum concentration improves amplifier spectral flatness in the C and L-bands and reduces the erbium pairing effect. Phosphorus doping further broadens the gain spectrum in the L-band. The erbium doping profile and fiber waveguide design determine the overlap between erbium ions and the optical mode field, thus therefore the saturation performance of the amplifier. This section reviews C and L-band spectral characteristics of EDF with different doping compositions and the change in spectral gain shape as a function of aluminum concentration and phosphorus doping.

2.1 Method to Determine Gain Spectrum

For quantitative EDF spectral evaluation, it is essential to have an accurate and repeatable method of predicting the gain shape in order to compare the spectral shape variation with different fiber parameters. EDF spectral gain shape is typically determined by two methods, amplifier measurement and fiber measurement. In the amplifier measurement, the spectral gain shape is measured in a designated amplifier configuration when the amplifier is operated at a required inversion and power level. Solid amplifier measurements require that test setup is carefully characterized and other conditions, such as fiber length, inversion level or gain tilt, input/output splice loss etc, are well controlled. In the fiber measurement, the fiber absorption with 0% erbium ion inversion and small signal gain with 100% erbium ion inversion are measured. The spectral gain is then calculated using average inversion method ⁽⁷⁾. Repeatable absorption and small signal gain measurements are critical for this method. The gain $G(\lambda)$ can be determined using the following equation by neglecting the fiber background loss.

$$G(\lambda, Inv) = [g^*(\lambda) \cdot Inv - (1 - Inv)\alpha(\lambda)]L \tag{1}$$

where $\alpha(\lambda)$ is the EDF absorption $\alpha(\lambda)$ and $g^*(\lambda)$ is the small signal gain at full inversion, L is the fiber length, and Inv is the average inversion.

We used average inversion method based on measured absorption and small signal gain for spectral comparison of different EDFs. Fig. 1 shows typical measured absorption and small signal gain, and Fig. 2 shows its corresponding gain spectrum. In the gain spectrum, appropriate fiber length and inversion level are determined to reach a minimum of 20dB near 1538nm and 1565nm.

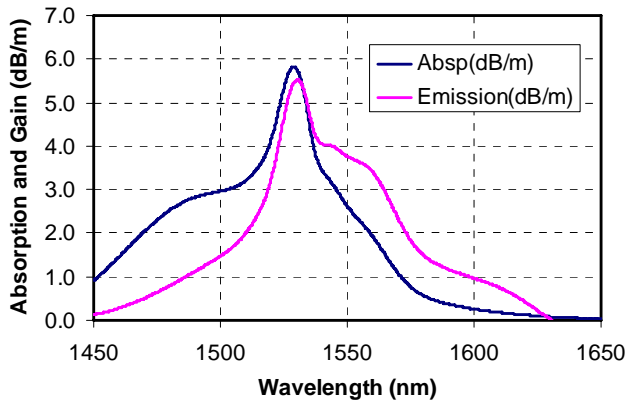


Fig. 1 Measured absorption and small signal gain

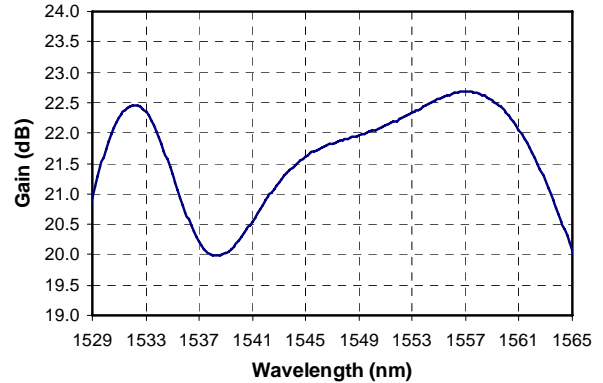


Fig. 2 Calculated gain shape with 20dB minimum gain near 1538nm and 1565nm

2.2 EDF Spectral Characteristics

EDF absorption and small signal gain are fundamental fiber spectral parameters. The absorption and small signal gain are determined by fiber absorption and emission cross-sections, overlap between optical field and erbium ions, and erbium concentration via following equations.

$$\alpha(\lambda) = \int_0^{2\pi} \int_0^{+\infty} \sigma_a(r, \lambda, \theta) \psi(r, \lambda) N(r, \theta) dr d\theta$$

$$g^*(\lambda) = \int_0^{2\pi} \int_0^{+\infty} \sigma_e(r, \lambda, \theta) \psi(r, \lambda) N(r, \theta) dr d\theta \quad (2)$$

where σ_a and σ_e are absorption and emission cross-sections of erbium ions, ψ is the normalized mode intensity distribution of the LP₀₁ mode, and N is the erbium ion concentration.

Both cross-sections and overlap are wavelength dependent. Spectral characteristics of absorption and emission cross-sections are determined by the host glass and dopant composition. The silica based EDF is typically co-doped with Al, Ge, and sometimes La, P and other codopants. Aluminum co-dopant is mostly used to improve the spectral flatness and to reduce the erbium pairing^{(8), (9)}. The overlap is also wavelength dependent because the optical field varies with wavelength.

In order to understand the relationship between aluminum concentration and the EDF spectral properties, EDFs with different aluminum concentration were made and measured. Fig. 3 shows the normalized absorption spectrum of three EDFs with different aluminum concentrations. The aluminum concentrations for fibers #1, #2, and #3 were about 6 M%, 12 M%, and 14 M%, respectively. It is apparent that with the increase of the aluminum level, the wavelength of the absorption peak shifts to a shorter wavelength and the absorption at 1480nm becomes higher relative to the absorption peak.

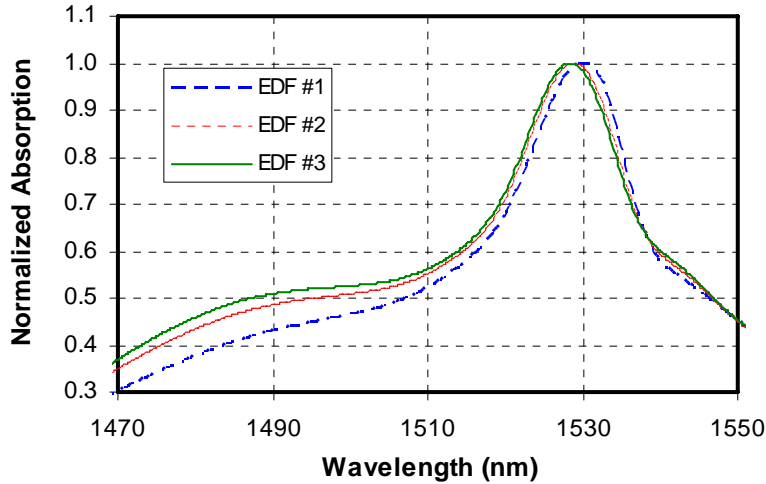


Fig. 3 Normalized absorption spectra with different Al concentrations
(EDF #1 – 6 mol%, EDF #2 – 12 mol%, EDF #3 – 14 mol%)

To examine the effect of aluminum concentration on EDF's spectral gain shape, the gain spectra of these three fibers were determined using equation (1). The spectral bandwidth used was 36nm from 1529nm to 1565nm and the flatness was optimized by selecting proper average inversion level to set zero tilt between minimum gains near 1538nm and 1565nm. An appropriate fiber length was chosen to achieve a minimum 20dB gain in each case. Gain spectra of these fibers are shown in Fig. 4. Comparison results confirm that higher aluminum concentration not only broadens the spectral bandwidth by shifting the 1532nm peak to a shorter wavelength but also reduces the gain peak near 1532nm

and thus improves the overall gain spectral flatness. In addition, the gain differences between EDF #1, #3 relative to fiber #2 are shown in Fig. 5. Increasing aluminum concentration has a significant effect on wavelengths shorter than 1550nm and most significantly near 1535nm. Its effect on wavelengths longer than 1550nm is relatively small.

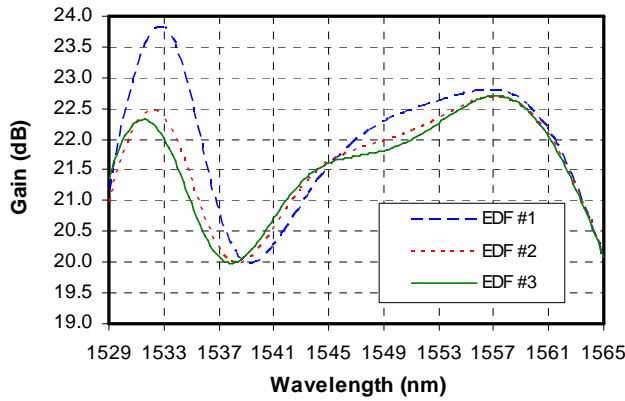


Fig. 4 Gain spectra of different EDFs in 36nm bandwidth (EDF #1 – 6 mol%, EDF #2 – 12 mol%, EDF #3 – 14 mol%)

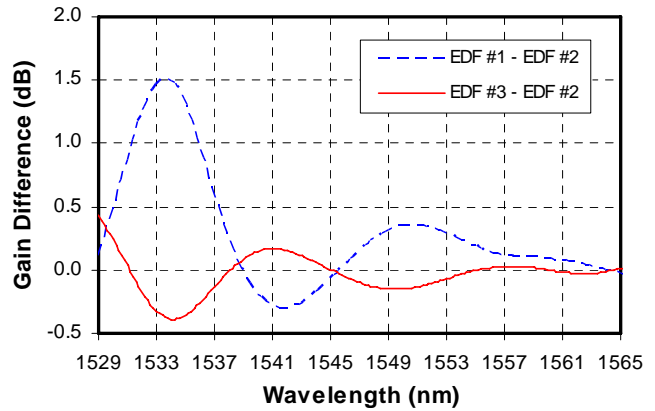


Fig. 5 Gain shape difference relative to fiber #2 (EDF #1 – 6 mol%, EDF #2 – 12 mol%, EDF #3 – 14 mol%)

For L-band comparison, the spectral gain shapes of both EDF #2 and EDF #3, shown in Fig. 6, are determined for wavelength from 1570nm to 1600nm. The minimum gain is 30dB in both cases. Gain ripples are 0.78dB and 0.86dB, respectively, for fiber #2 and fiber #3. Again, higher aluminum concentration results in a flatter gain shape in L-band.

Adding different co-dopants usually lead to different fiber spectral characteristics. Sometimes, it is useful to expand the gain spectrum beyond 1600nm or even 1610nm to increase channel counts or amplifier bandwidth. It has been demonstrated ⁽¹⁹⁾ that adding phosphorus improves the spectral flatness beyond 1600nm. A typical spectral comparison between EDF #3 and phosphorus co-doped EDF, EDF #4, for wavelength between 1575nm and 1620nm in extended L-band is shown in Fig. 7. The result shows that P codoped EDF has significantly improved EDF gain flatness beyond 1605nm wavelength. The gain ripple for the EDF #4 is about 4dBm at a 25dB minimum gain for wavelength between 1575nm and 1620nm.

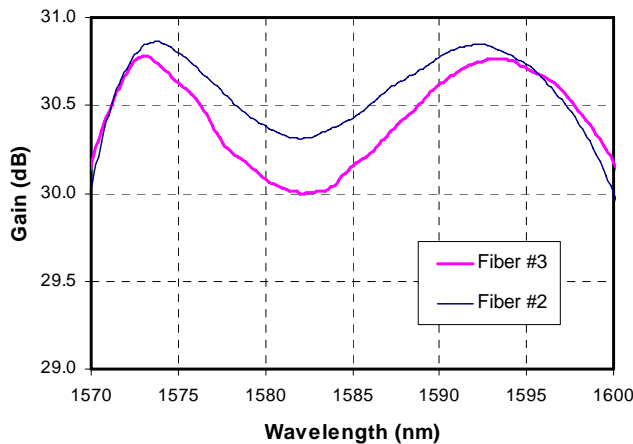


Fig. 6 Gain spectrum comparison in L-band region

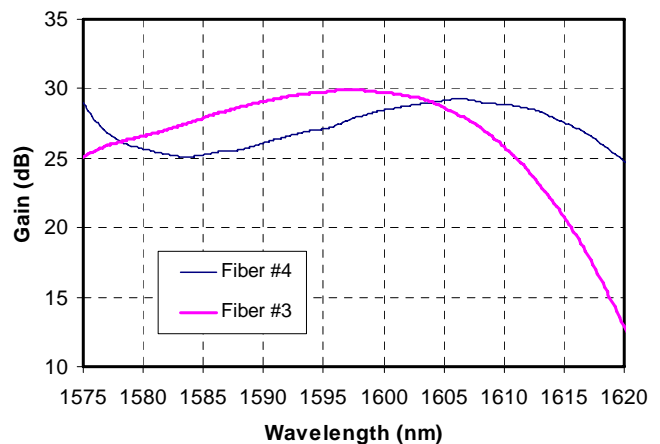


Fig. 7 Gain spectrum comparison in extended L-band region between Al co-doped EDF (#3) and P co-doped EDF (#4)

3. HIGH POWER APPLICATIONS

For high power applications, large mode area fiber with low numerical aperture lowers pump intensity, thereby reducing nonlinear effects, such as 980nm pump excited state absorption which limits the power conversion efficiency at high power ^{(2), (11), (12)}. In addition, it is desirable to maintain flat spectral gain shape, which requires high aluminum concentration. However, aluminum raises fiber refractive index and this leads to high NA. For low NA fiber, the aluminum concentration generally needs to be compromised.

In this section, a novel erbium doped fiber design is described, which offers not only large mode area with low NA to reduce nonlinear effect, but also high aluminum content to improve gain spectral flatness. The design and optical characteristics of the high power EDF and the effect of fiber numerical aperture on power conversion efficiency are illustrated. We also present some experimental comparison results with other EDFs on spectral flatness, efficiency and spliceability. In addition, another high power output option (>27dBm) with combination of EDF and Er/Yb double cladding fiber is discussed.

3.1 High power Erbium Doped Fiber Design

An optimal EDF for high power applications requires proper design of fiber doping composition and waveguide. The typical EDF design with high NA and confined erbium ion distribution is more beneficial for low power applications. For high power applications pumped at 980nm, it is known that excited state absorption (ESA) from the ⁴I_{11/2} significantly affects the efficiency of EDFAs. Lower NA reduces this non-linear effect and improves power conversion efficiency.

In order to quantitatively describe the high power EDF design, an EDFA model based on work by Giles et. al. ⁽⁷⁾ is used to determine the effect of fiber waveguide parameters on the amplifier performance in the high power region. Additional loss mechanisms, such as 980nm pump ESA and the erbium ion clustering effect, are also included in the model ^{(9), (10)}. The loss mechanism of 980nm pump ESA is modeled by adding an additional upper level for the pump ESA with population n_3 and introducing the pump excited state absorption $\alpha_{pump}^{ESA}(\lambda)$ to the pump power propagation equation. In the simulation, the corresponding fiber modeling parameters for the different fiber design are firstly determined. Then the power conversion efficiency (PCE) defined in equation (3) is calculated at different pump power levels.

$$PCE = \frac{P_{out}^s - P_{in}^s}{P_{in}^p} \tag{3}$$

where P_{in}^s is the input signal power, P_{out}^s is the output signal power, and P_{in}^p is pump power injected into the EDF.

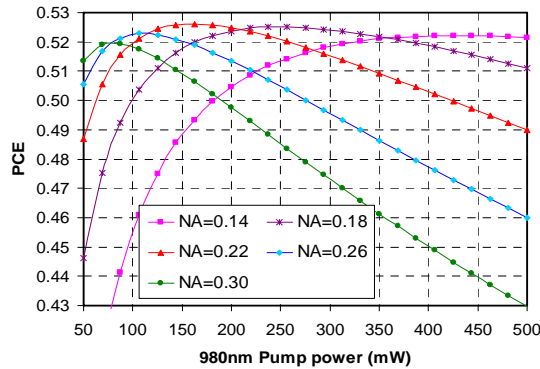


Fig. 8 PCE vs. pump power for different fiber NAs with 980nm pumping

Fig. 8 shows the modeling result of PCE versus launched 980nm pump power. In the simulation, the erbium distribution is assumed to be flat-top and has same radius of fiber core. The fiber is assumed to have a step index core. We only vary numerical aperture of the fiber. All other fiber parameters are kept the same. The input signal power is 0dBm at 1550nm wavelength and the 980nm pump co-propagates with signal. At each pump power level, fiber length is optimized to achieve maximum output signal power.

The simulation result shows that EDF efficiency strongly depends on fiber numerical aperture at different pump power levels. Low NA fiber is beneficial for high power applications, whereas high NA fiber is more suitable for low power applications. For different applications, the EDF needs to be properly designed to achieve optimal performance.

The fiber cutoff wavelength is another critical factor that affects the fiber performance. Higher cutoff improves the overlap between erbium ions and the optical mode field. Fig. 9 shows power conversion efficiency for two different fiber designs with different NA and fiber cutoff wavelengths. The fiber parameters used in the calculation are shown in Table 1. The peak efficiency difference between these two fibers is mainly attributed to erbium concentration difference. The result also shows that the fiber of design #2 has better efficiency than that of design #1 in high power region. The efficiency difference is over 10% at 500mW pump power level.

Table 1 Fiber parameters of two different fiber designs

	Design #1	Design #2	Unit
Er peak absorption around 1530nm	6.5	6.5	dB/m
Numerical aperture	0.22	0.18	
Cutoff wavelength	900	1100	nm

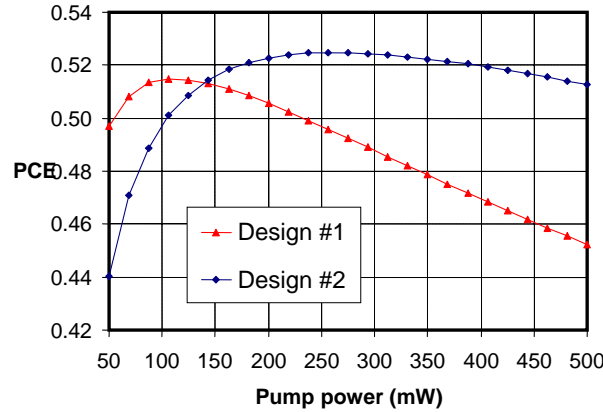


Fig. 9 PCE for two different fiber designs (simulated)

3.2 Experimental Result

Based on the above design, we developed a new high power EDF (Fiber #5) with NA and cutoff around 0.18 and 1100nm, respectively. Fiber parameters are shown in Table 2.

This fiber also has high aluminum concentration through a new EDF manufacturing process via MCVD. The aluminum concentration of the fiber is estimated to be around 13 mol%. To evaluate the gain spectral shape characteristics, we measured the absorption $\alpha(\lambda)$ and small signal gain $g^*(\lambda)$ of this fiber and determine the spectral gain shape using average inversion method. The gain shape comparison with other two commercial EDFs, Fiber #1 and Fiber #2 discussed in section 2, is shown in Fig. 10. The aluminum concentration of Fiber #1 and Fiber #2 is about 6 mol% and 12 mol%, respectively. The numerical aperture of Fiber #1 and Fiber #2 is 0.23 and 0.18, respectively. As shown in the graph, the new high power fiber has about 1dB flatness improvement over its low NA counterpart, Fiber #1 and slightly better flatness than Fiber #2.

Table 2 Characteristics of new high power EDF

	High Power EDF	Unit
Peak absorption around 1530nm	7.4	dB/m
Pump peak absorption around 980nm	4.0	dB/m
Background loss at 1550nm	0.5	dB/km
Numerical aperture	0.176	
Cutoff wavelength	1140	nm
Mode field diameter @ 1550nm	6.7	μm
Estimated aluminum concentration	13	mol%

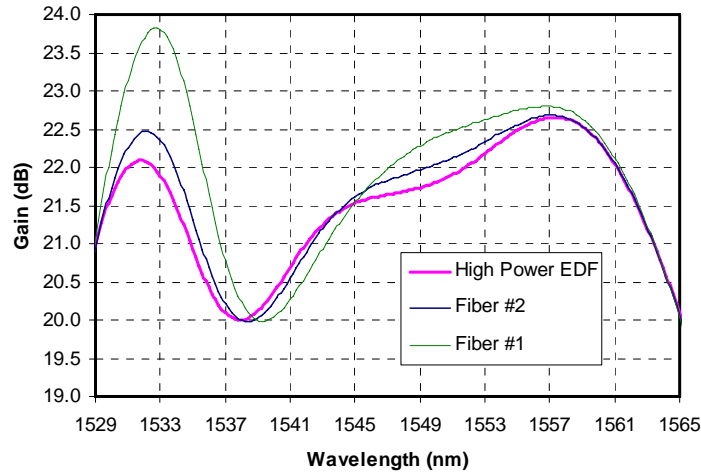


Fig. 10 Comparison of gain flatness of the new high power EDF with Fiber #1 and Fiber #2

To evaluate the new fiber’s actual performance, we measured its power conversion efficiency and compared with Fiber #2. In the measurement, a one-stage amplifier configuration with co-propagating pump was used. The maximum output pump power is 600mW at around 980nm. The input signal wavelength is 1550nm and the signal power is 0dBm. In the measurement, input and output splice losses were also measured and taken into account in the efficiency calculation. The experimental efficiency result shown in Fig. 11 clearly indicates that new fiber outperforms Fiber #2 for pump power over 150mW. The experimental result agrees well with the simulation result shown in the preceding section. The efficiency of the new fiber is about 0.6dB better than that of Fiber #2 at 600mW pump power.

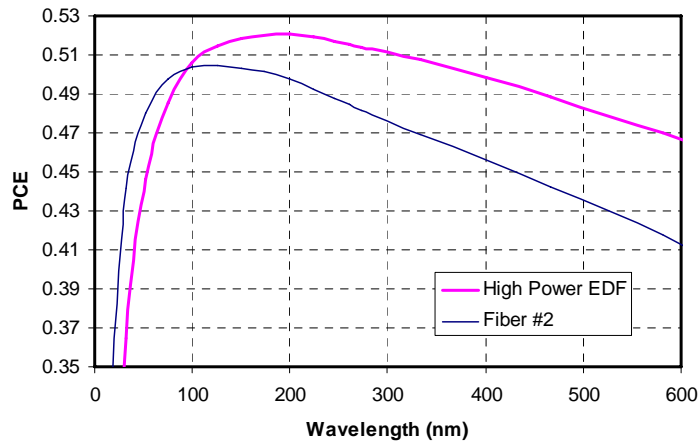


Fig. 11 Measured PCE vs. launched pump power for two fibers with 0dBm and 1550nm signal input

We also evaluated spliceability of this new fiber to typical pigtail fibers using an Ericsson #995 splicer and compared with Fiber #2. A comparison result of their typical splice loss to SMF28 at different wavelength is shown in Fig. 12. The splice loss was measured and optimized at 1305nm. Compared to Fiber #2, the splice loss of the high power EDF is improved and wavelength dependency is reduced.

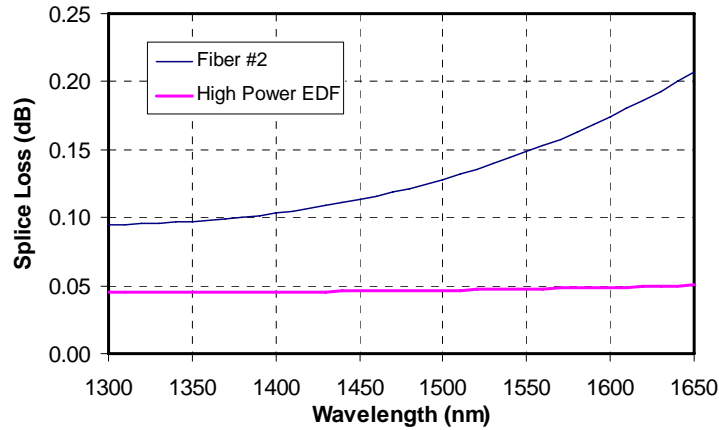


Fig. 12 Spectral characteristics of splice loss to SMF28

3.3 Er/Yb DCF for High Power Application

Erbium doped fiber is generally not a cost-effective solution for high output (>27dBm) applications mainly because of the high cost of high power SM pumps. EDF co-doped with ytterbium (Er/Yb fiber) provides an alternative solution for high power applications^{(13), (14)}. The ytterbium has a broad absorption spectrum about 200nm around 900nm. Typical pump wavelengths that can be used are 915nm, 975nm, 800nm, and 1060nm. In addition, the cladding-pump fiber design with dual cladding makes it possible to use high power MM pump diodes and emitters. For the ytterbium co-doped EDF, pump photon is absorbed by the ytterbium ions and is excited to the upper state. The energy is transferred to the upper state of erbium ions, which then decay to ground state to produce amplification.

For WDM application, Er/Yb codoped fiber does not produce as flat a gain spectrum as EDF. So Er/Yb fiber is suited for narrow band or single channel application. Hybrid use of EDF and Er/Yb fiber with latter used in the second power stage reduces the spectral limitation of the Er/Yb fiber. An example of combined gain spectrum and corresponding fiber gain spectra is shown in Fig. 13. EDF and Er/Yb fiber are used for first and second amplifier stages, respectively. The EDF in the first stage produces about 20dB gain, and the Er/Yb fiber in the second stage generates about 10dB gain. This results in a combined minimum gain of 30dB and gain ripple of 4.5 dB for wavelength from 1533nm to 1565nm. The total signal output power is over 27dBm.

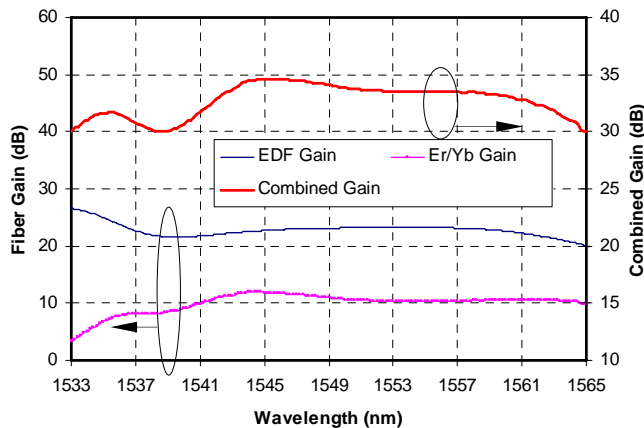


Fig. 13 Combined gain spectrum using EDF and Er/Yb fiber

4. OTHER EDF TOPICS

4.1 EDF Temperature Characteristics

Modern WDM systems require that the gain shape is well controlled over a certain temperature range. However, the spectral gain shape of EDF exhibits temperature dependence in both C-band and L-band region. This is attributed to the variation in occupational probability densities of erbium ions in each of the 56 manifold between excited (metastable) and ground states. As a result, the EDF absorption $\alpha(\lambda)$ and small signal gain $g^*(\lambda)$ defined in equation (2) are temperature dependent. The population inversion is also temperature-dependent because of power evolution and saturation power variation for different temperatures.

The EDF temperature characteristics can be accurately modeled by determining corresponding absorption $\alpha(\lambda)$ and small signal gain $g^*(\lambda)$ for different temperatures ⁽¹⁵⁾. The following fitting expression can be used to generate modeling parameters at a different temperature T with known or measured parameters at T_0 .

$$\alpha(\lambda, T) = \alpha(\lambda, T_0) \exp\left[\beta_a \left(\frac{1}{kT} - \frac{1}{kT_0}\right)\right]$$

$$g^*(\lambda, T) = g^*(\lambda, T_0) \exp\left[\beta_g \left(\frac{1}{kT} - \frac{1}{kT_0}\right)\right] \quad (4)$$

where β_a and β_g are wavelength dependent empirical fitting parameters, which can be determined by measuring $\alpha(\lambda)$ and $g^*(\lambda)$ at different temperatures, and k is the Boltzmann's constant.

Experimental WDM gain measurement was made to compare the gain shape variation with this modeling approach for two different temperatures 20°C and 60°C. Both the average gain for these two temperatures and gain difference between these two temperatures are shown in Fig. 14. The result shows a good agreement between the established model and the experiment. The difference is less than 0.06dB from wavelength range from 1531nm to 1565nm.

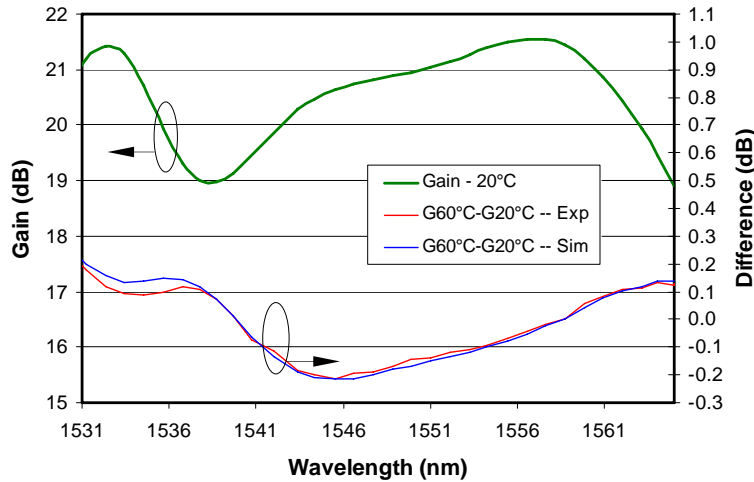


Fig. 14 Comparison of temperature induced gain shape change between modeling and experiment (20°C and 60°C)

To suppress the temperature induced gain variation, the EDF temperature is usually actively controlled. However, it is desirable to compensate this gain shape change passively. It has been demonstrated that a hybrid method combining standard Al codoped EDF with Sb codoped EDF can reduce EDF temperature dependency in the 1545nm range ⁽¹⁶⁾. Antimony (Sb) codoped EDF shows opposite temperature variation compared to standard Al codoped EDF in wavelength range around 1530nm and 1550nm. Combined use of Sb codoped EDF and standard EDFs reduces the temperature variation of amplifiers.

4.2 980nm Pump Induced Effect

It has been shown that 980nm pump wavelength has a significant effect on EDFA's spectral gain shape^{(17), (18)}. Pump wavelength change leads to spectral gain shape variation, which affects output spectral flatness. This inhomogeneous feature is associated with erbium ion site-to-site variation of each manifold in $^4I_{13/2} \rightarrow ^4I_{15/2}$ transition. However, a fully inverted amplifier does not seem to be pump wavelength dependent. For C-band EDFAs, the effect is mostly on wavelength shorter than 1540nm, and the effect is small for wavelength between 1540nm and 1565nm.

A typical measurement result of gain spectral variation for different 980nm wavelengths is shown in Fig. 15. The amplifier measurement was made using WDM C-band input signals with 100GHz spacing and wavelength range from 1527nm to 1565nm. The composite power of input signal was 0dBm. The single-stage amplifier was co-pumped with a wavelength tunable 980nm pump. The average gain spectrum and the gain difference between two adjacent pump wavelengths are shown. Average wavelengths for the measurements were 975.1nm, 975.6nm, 976.1nm, and 979.8nm, respectively. Corresponding wavelength changes are 0.49nm, 0.55nm, 0.43nm, and 0.42nm, respectively at these wavelengths. The result shows that 980nm pump wavelength needs to be tightly controlled and the effect can be mitigated using shorter wavelength pumps or combing 980nm pumps with different wavelengths.

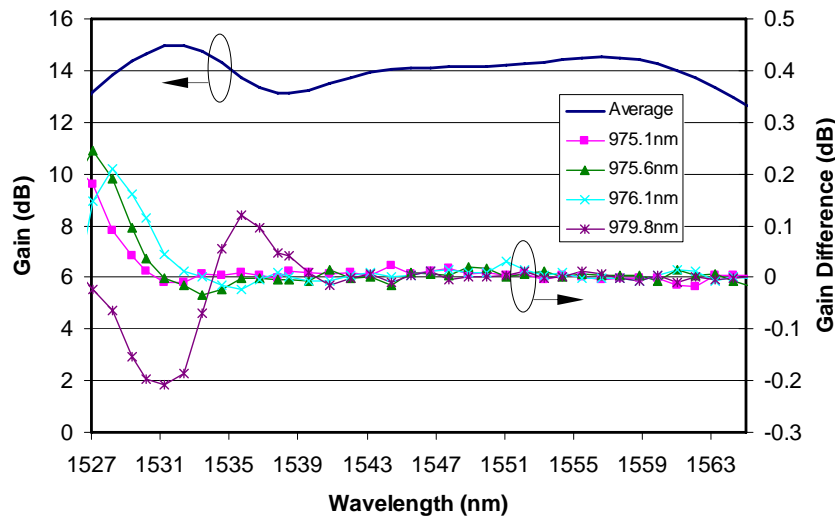


Fig. 15 Experimental result of spectral shape change with different 980nm pump wavelengths

5. CONCLUSIONS

We have reviewed the status and some recent progress of erbium doped fibers for high performance amplifiers. Spectral characteristics of EDFs with different doping compositions have been quantitatively described. For high power applications, EDF with low NA and high aluminum concentration improves amplifier efficiency and performance and reduces non-linear effect. For even higher power applications (>27dBm), hybrid use of selected EDF and Er/Yb double cladding fiber offers a viable solution. Various EDF topics on EDF impairment have been discussed with simulation and experimental examples.

6. REFERENCES

1. J. L. Zyskind, J. A. Nagel, and H. D. Kidorf, "Erbium-doped fiber amplifiers for optical communications," Optical Fiber Telecommunications IIIB, ed. I. P. Kaminow and T. L. Koch, 13 (1997)
2. P. F. Wysocki, "Erbium-doped fiber amplifiers: advanced topics," Rare-Earth-Doped Fiber Lasers and Amplifiers, ed. M. J. Digonnet, 583 (2001)

3. W. Miniscalco, "Erbium-doped glasses for fiber amplifiers at 1500nm," *IEEE J. Lightwave Technol.* **9**, 234 (1991)
4. W. J. Miniscalco and R. S. Quimby, "General procedure for the analysis of Er^{3+} cross-sections," *Opt. Lett.*, **16**, 258 (1991)
5. W. L. Barnes, R. I. Laming, E. J. Tarbox, P. R. Morkel, "Absorption and emission cross-sections of Er^{3+} -doped silica fibers," *IEEE J. Quantum. Electron.*, **27**, 1004 (1991)
6. B. S. Wang, G. Pub, R. Osnato, and B. Palsdottir, "Characterization of gain spectral variation of Erbium-doped fibers codoped with aluminum," *SPIE Proc.* **5280**, 161 (2003)
7. C. R. Giles and E. Desurvire, "Modeling erbium-doped fiber amplifiers," *J. Lightwave Technol.*, **9**, 271 (1991)
8. D. Gloge, "Weakly guiding fibers," *Appl. Opt.*, **10**, 2252 (1971)
9. P. Myslinski, D. Nguyen, and J. Chrostowski, "Effects of Concentration on the Performance of Erbium-Doped Fiber Amplifiers," *J. of Lightwave Technol.*, **15**, 112 (1997)
10. P.F. Wysocki, J.L. Wagener, M.J.F. Digonnet, and H.J. Shaw, "Evidence and modeling of paired ions and other loss mechanisms in erbium-doped silica fibers," *Proc. SPIE, Boston, Mass.* (1992)
11. J. C. Livas, S. R. Chinn, E. S. Kintzer, D. J. DiGiovanni, "High power erbium-doped fiber amplifier pumped at 980nm," in *Conference on Lasers and Electro Optics*, 15, 521, OSA Technical Digest Series, Optical Society of America, Washington, D.C. (1995)
12. B. Wang, G. Pub, and M. Andrejco, "Novel erbium doped fiber for high power applications," *SPIE Proc.* **5623**, (2004)
13. W. L. Barnes et. al, " Er^{3+} -- Yb^{3+} and Er^{3+} doped fiber lasers," *J. Lightwave Technol.*, **7**, 1461 (1989)
14. J. E. Townsend et. al, " Yb^{3+} sensitized Er^{3+} doped silica optical fiber with ultrahigh transfer efficiency and gain," *Electron. Lett.*, **27**, 1958 (1991)
15. P. F. Wysocki, "Simple modeling approach for the temperature dependence of the gain of erbium-doped fiber amplifiers," *Optical Devices for Fiber Communication, Proc. SPIE* **2847**, (2000)
16. U. C. Ryu, K. Oh, D. J. DiGiovanni, B. S. Wang, A. Hariharan, "Suppression of temperature-dependent gain variation of conventional EDFA by hybrid connection of antimony-doped silica EDF," *Electron. Lett.*, **39**, 975 (2003)
17. M. J. Yadlowsky, "Pump wavelength-dependent spectral-hole burning in EDFAs," *J. of Lightwave Technol.*, **17**, 1643 (1999)
18. F. A. Flood, and C. C. Wang, "980-nm pump-band wavelengths for long-wavelength-band erbium-doped fiber amplifiers," *IEEE Photonics Technology Letters*, **11**, 1232 (1999)
19. I. P. Byriel, B. Pálsdóttir, M. Andrejco, C.C. Larsen, "Silica based erbium doped fiber extended the L-band to 1620+ nm," *ECOC 2001, Tu L 3.5* (2001)